CHAPTER 6

RESULTS AND DISCUSSION (PART III):

COMPARISON OF (1-*x*)PZT–*x*DOPED BIT SYSTEM

In this research, (1-*x*)PZT–*x*doped BIT ceramic systems were prepared and characterized. The results revealed that the dielectric properties, ferroelectric properties and fatigue behavior of new ceramic systems were improved. This research attempted to combine the fatigue-free properties of doped-BIT and superior dielectric and ferroelectric properties of PZT together, in agreement with other previous works [23-26]. In the case of doped $Bi_4Ti_3O_{12}$ material, it is commonly known that doping with suitable elements at the Bi-site or Ti-site in the perovskite-type unit of $Bi_4Ti_3O_{12}$ can effectively optimize the ferroelectric properties. Hence, many researchers studied the effect of different-site doping on the properties of $Bi_4Ti_3O_{12}$. Recent studies revealed that Bi^{3+} ions in $Bi_4Ti_3O_{12}$ structure could be substituted by donor doping in Bi-site with La [3, 8, 23-26], Dy [9, 10], Sm [11], Nd [12] or Pr [13] (trivalent lanthanide ions) and in the Ti-site with Nb [14-17], V [18] or W [19] for the improvement of its ferroelectric properties. It has been suggested that the Bi and Ti-sites doping had different effects on the ferroelectric properties. Therefore, (1-*x*)PZT–*x*doped BIT which different-site doping at Bi-site (BDT) and Ti-site (BNbT) may represent different ferroelectric properties as well. In this chapter, we would like to compare the properties of newly fabricated (1-*x*)PZT–*x*BDT and (1-*x*)PZT–*x*BNbT ceramics system.

6.1 Comparison of phase evolution between PZT–BDT and PZT–BNbT systems

From the comparison of X-ray diffraction patterns between (1-*x*)PZT–*x*BDT and (1-*x*)PZT–*x*BNbT ceramics, the results revealed that the pattern of PZT ceramic showed tetragonal phase which could be matched with ICSD file number 92059 of $Pb(Zr_{0.52}Ti_{0.48})O_3$ [102]. While BDT and BNbT ceramics were identified as a single-phase material having an orthorhombic structure accordance with $Bi_4Ti_3O_{12}$ (BIT) structure and could be matched with ICSD file number 87810 of $Bi_4Ti_3O_{12}$ (BIT) [106]. The correlation of the diffraction peaks of the doped-BIT (BDT and BNbT) with BIT phase implied that ions-substitution did not affect the layered-perovskite like structure of $Bi_4Ti_3O_{12}$. This indicated that the Dy and Nb ions in the BIT ceramics did not form pyrochlore or secondary phases but were dissolved into the pseudo-perovskite structure of bi-layered perovskite structure. This suggested that Dy^{3+} and Nb^{5+} could be readily substitute for Bi^{3+} (Bi-stie) and Ti^{4+} (Ti-site) ions in pseudo-perovskite structure, respectively.

Addition of small amount of doped-BIT into PZT (i.e. 0.9PZT–0.1BDT and 0.9PZT–0.1BNbT), the tetragonal structure of PZT was maintained with all peaks shifted to the right. The 0.9PZT–0.1BDT patterns appeared the main peak (117 at 2θ ~ 29.5°) of BIT while 0.9PZT–0.1BNbT did not present as shown in Figure 6.1. This result revealed that at this composition (x = 0.1), BNbT phase completely dissolved into PZT phase. Addition of doped-BIT content to 30 wt% (0.7PZT–0.3BDT and 0.7PZT–0.3BNbT), peaks of PZT phase was maintained while some peaks of $Bi_4Ti_3O_{12}$ phase appeared. Increasing of 50 wt% doped-BIT (0.5PZT–0.5BDT and 0.5PZT–0.5BNbT), two systems showed different X-ray diffraction patterns. The 0.5PZT–0.5BDT ceramic showed mixture between tetragonal phase of PZT and

orthorhombic phase of $Bi_4Ti_3O_{12}$. While, orthorhombic phase of BIT was dominated in 0.5PZT–0.5BNbT composition. When, more doping content of $Bi_4Ti_3O_{12}$ ($x > 0.5$) was added, the patterns of both ceramic systems (PZT–BDT and PZT–BNbT) showed orthorhombic distortion of $Bi_4Ti_3O_{12}$ phase. For the (1-*x*)PZT–*x*BDT system (when $x = 0.3$-0.9), small amount of second phase correlating with $Pb_2Bi_4Ti_5O_{18}$ compound (matched with ICSD file number 150403 [110]) could be detected as shown in Figure 6.1. However, for the (1-*x*)PZT–*x*BNbT (when $x = 0.3$-0.9) no second phase presented but some peaks due to reflection of distorted lattice were observed as shown in Figure 6.1. From the comparison of X-ray diffraction patterns between PZT–BDT and PZT–BNbT ceramics, it seemed that dissolubility of BNbT into PZT was higher than that of BDT. This result can be attributed to the dissolubility of additive affected due to size of ionic radius, number of valency atom and site of dopant substituted.

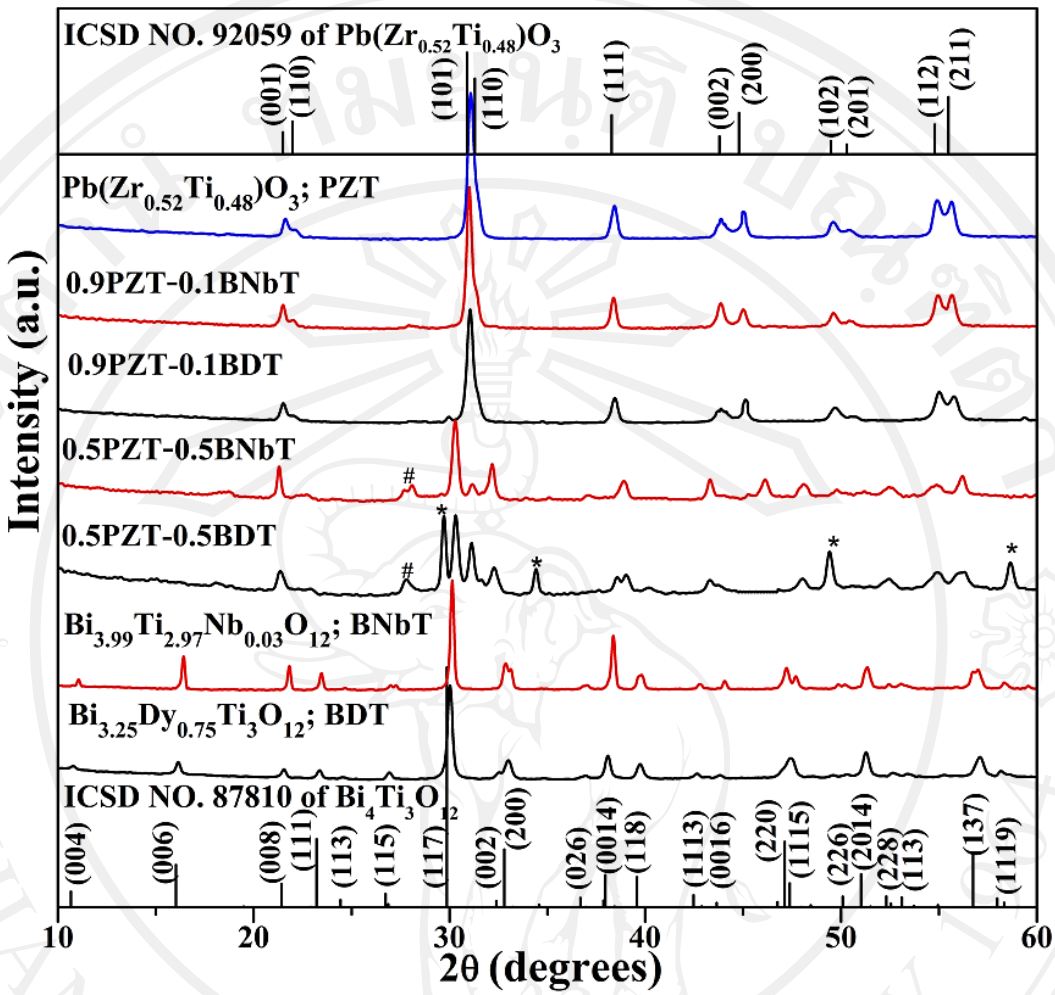

Figure 6.1 Comparison of X-ray diffraction pattern between (1-*x*)PZT–*x*BDT and (1-*x*)PZT–*x*BNbT, when *x* = 0, 0.1, 0.5 and 1.0; * and # are defined as second phase ($Pb_2Bi_4Ti_5O_{18}$ compound) and unknown peaks, respectively.

6.2 Comparison of physical properties between PZT–BDT and PZT–BNbT systems

Figure 6.2 shows comparison of microstructure between (1-*x*)PZT–*x*BDT and (1-*x*)PZT–*x*BNbT ceramics sintered at 1000°C for 4 h with a heating/cooling rate 5°C/min. Both BDT and BNbT ceramic had plate-shape grains. Addition of 10 and 30 wt% doped-BIT, the grain size decreased rapidly, however, equiaxed grains still obtained. The plate-like grains were dominated at the same composition (x = 0.5) for both systems i.e. 0.5PZT–0.5BDT and 0.5PZT–0.5BNbT. The 0.5PZT–0.5BDT ceramic showed combined microstructure between equiaxed and plate-like grains, while 0.5PZT–0.5BNbT showed only plate shape grains. This result correlated to X-ray diffraction pattern where the 0.5PZT–0.5BDT composition had mixed phases. Increasing of doped-BIT content, the plate-like grains were obtained for both systems.

Densification of (1-*x*)PZT–*x*BDT and (1-*x*)PZT–*x*BNbT ceramics were compared as shown in Figure 6.3. The densities of both ceramic systems showed similar trends. The highest densities of both systems were obtained at x = 0.1 (0.9PZT–0.1BDT and 0.9PZT–0.1BNbT). Further increase the content of doped-BIT (BDT or BNbT) gradually decreased densities of ceramics. This result was found to correlate to the microstructure. The reason could be explained that the composition contained plate-like grains which could have different orientation of plate stacking, resulting in higher concentration of pores and lower densities.

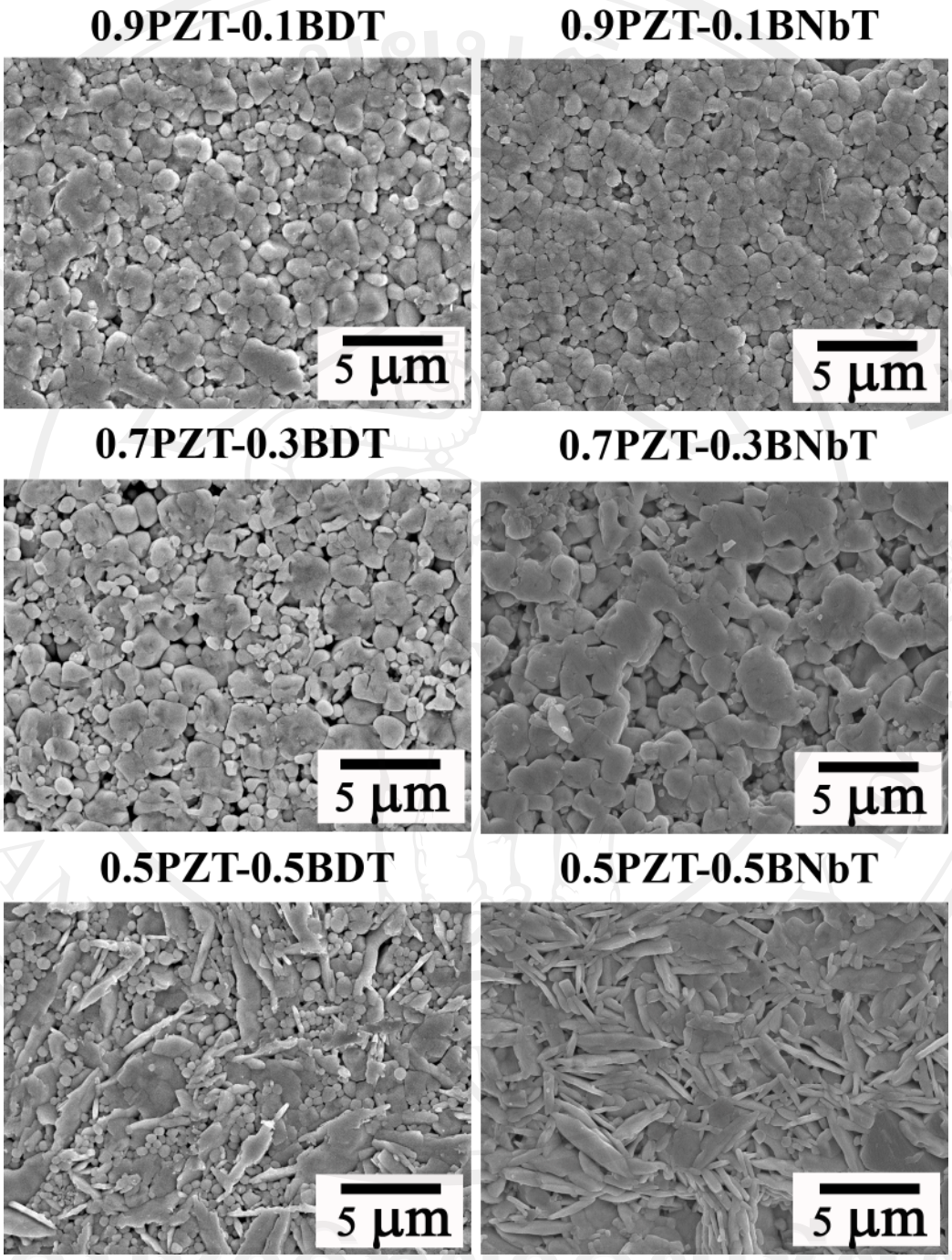

Figure 6.2 Comparison of microstructure between (1-*x*)PZT–*x*BDT and (1-*x*)PZT–*x*BNbT sintered at 1000°C.

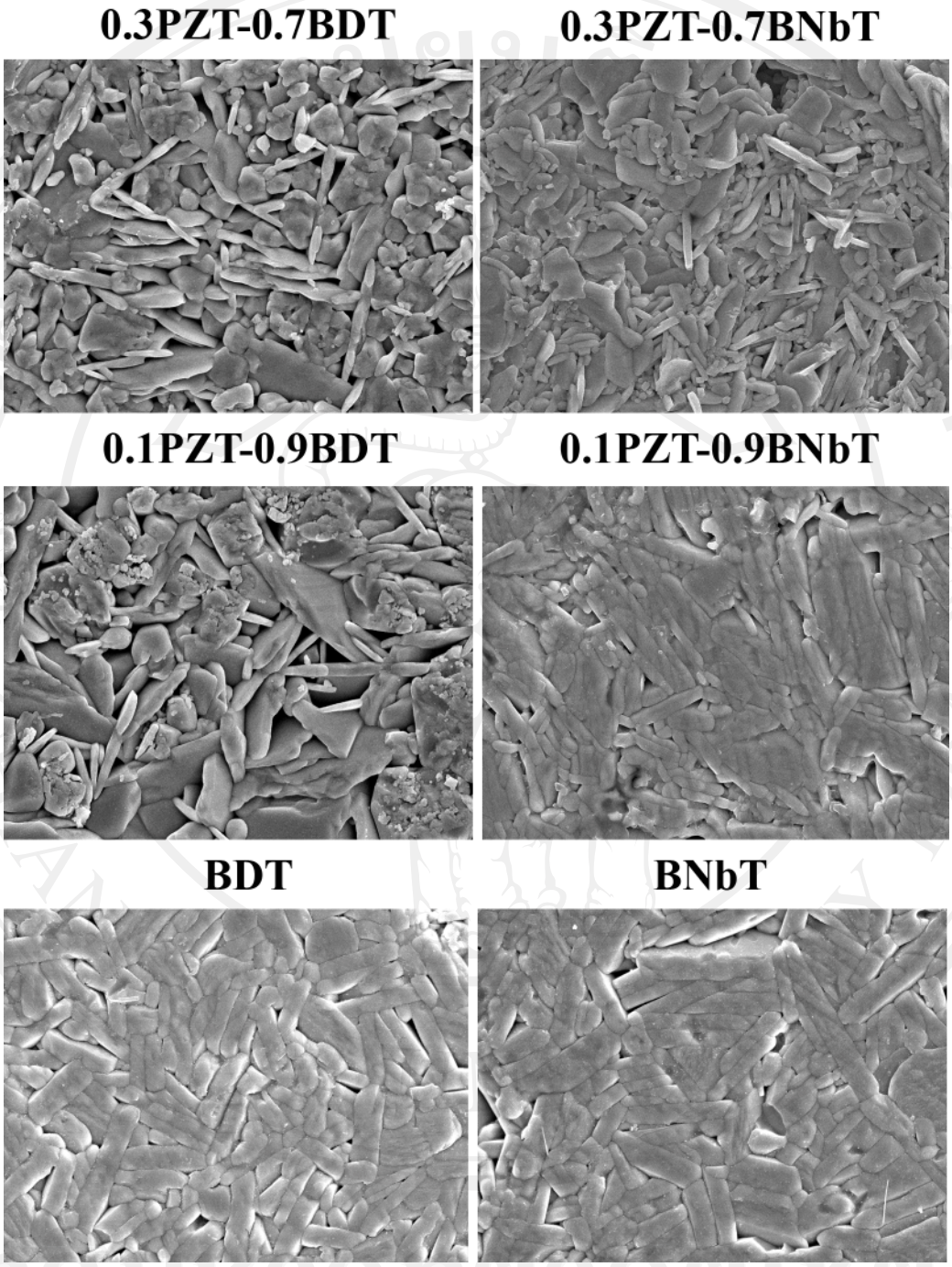

Figure 6.2 (continued) Comparison of microstructure between (1-*x*)PZT–*x*BDT and (1-*x*)PZT–*x*BNbT sintered at 1000°C.

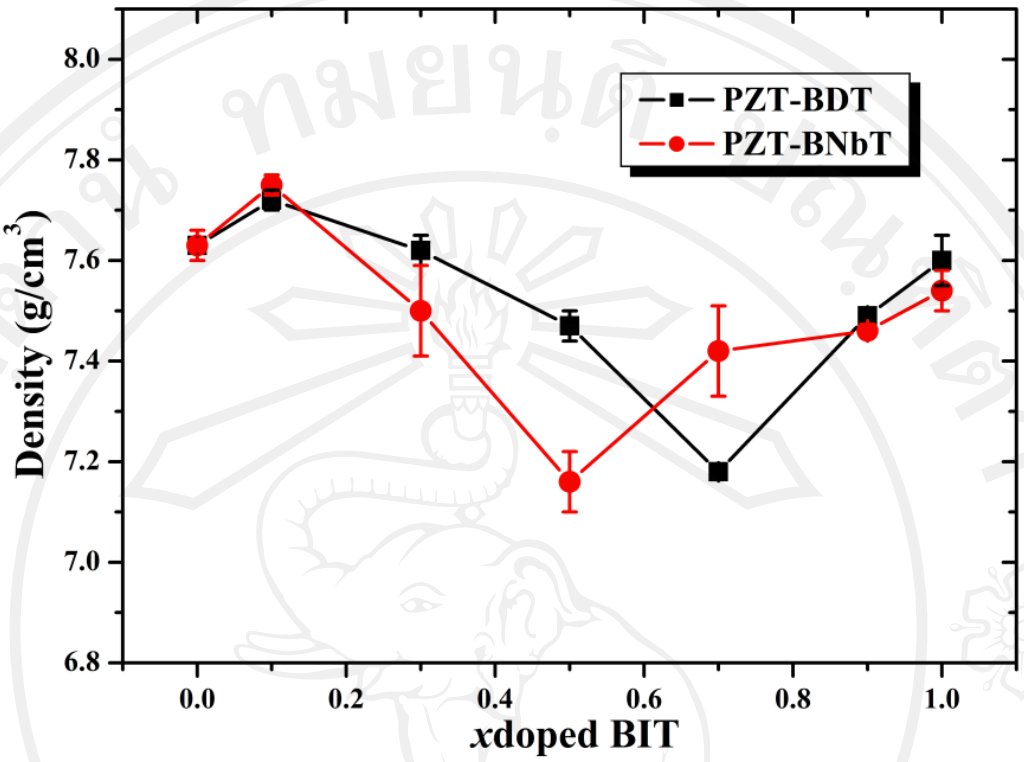

Figure 6.3 Comparison of densification between (1-*x*)PZT–*x*BDT and (1-*x*)PZT–*x*BNbT sintered at 1000°C.

6.3 Comparison of dielectric properties between PZT–BDT and PZT–BNbT systems

The comparison of dielectric properties between (1-*x*)PZT–*x*BDT and (1-*x*)PZT –*x*BNbT systems were investigated as shown in Figure 6.4(a) and (b). Both systems showed similar trend of dielectric properties. In the case of dielectric constant, an addition 10 wt% doped-BIT reduced the dielectric constant for both systems. This result could be explained by a reduction of grain size which affected domain clamping that led to low dielectric constant in the samples. Increasing of doped-BIT content, the dielectric constant of the ceramic further decreased gradually as shown in Figure 6.4(a). This result could be affected by an addition of too low dielectric material

(BDT or BNbT) in the system. When comparison between (1-*x*)PZT–*x*BDT and (1-*x*)PZT–*x*BNbT systems, the result revealed that the PZT–BNbT system exhibited higher dielectric constant value than PZT–BDT system. This result could be attributed to the second phase presented in PZT–BDT system which seemed to play a role in lower dielectric constant of ceramic. Figure 6.4(b) showed the dielectric loss of PZT–BDT and PZT–BNbT systems. The highest dielectric loss was achieved at $x = 0.5$ composition for both ceramic systems. The lowest density and heterogeneous microstructure in this composition seemed responsible for these high dielectric loss values. Comparison of dielectric loss between BDT and BNbT ceramics showed that the BNbT had lower value than that of BDT. This result could be affected by dopant tend to have a similar features compared with the other report [136, 137]. It could be implied that Nb-doping in $Bi_4Ti_3O_{12}$ led to a decrease space charge density thus decrease in dielectric loss.

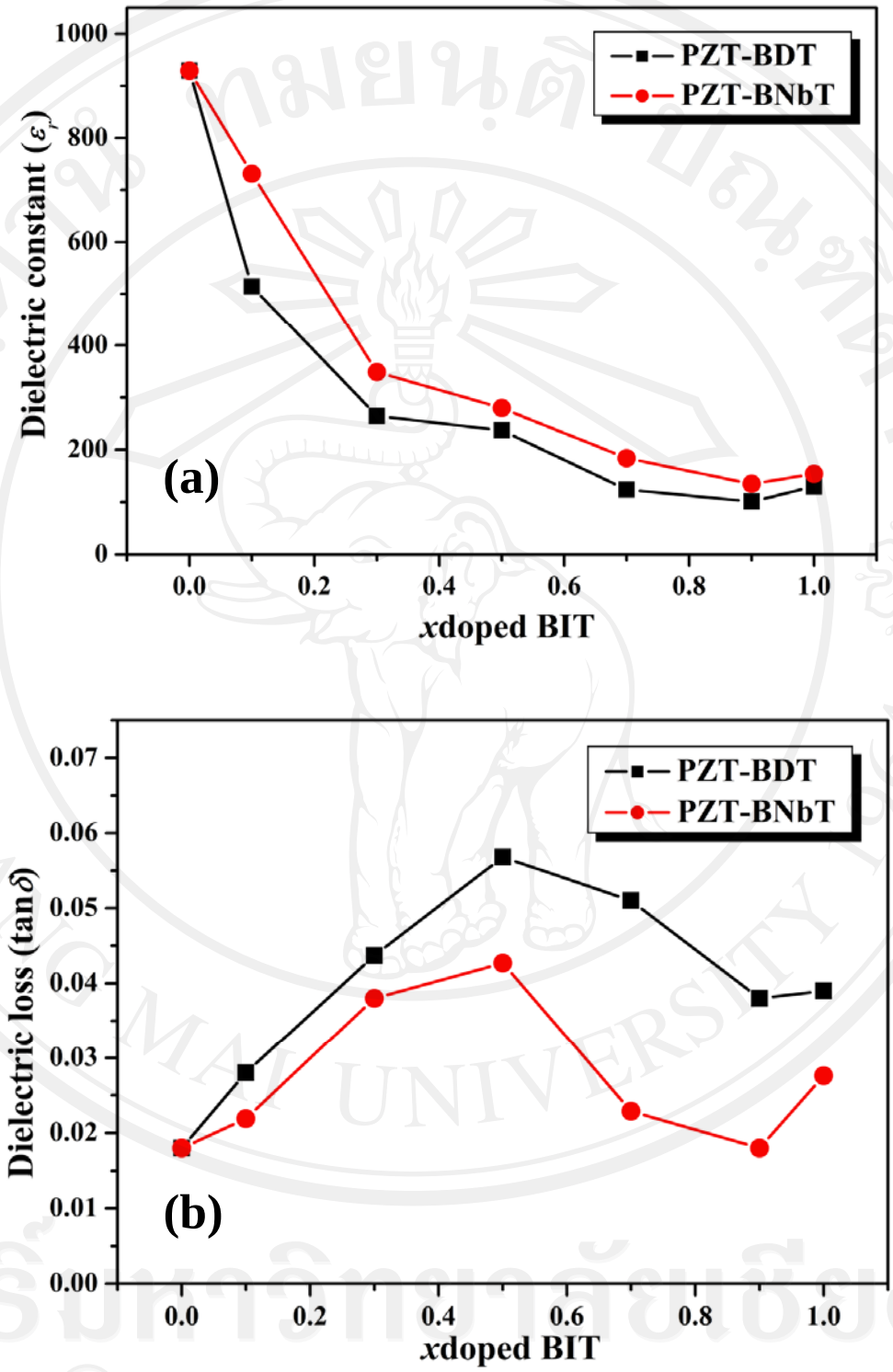

Figure 6.4 Comparison of dielectric properties (a) dielectric constant and (b) dielectric loss between (1-*x*)PZT–*x*BDT and (1-*x*)PZT–*x*BNbT systems.

6.4 Comparison of ferroelectric properties between PZT–BDT and PZT–BNbT systems

Figure 6.5(a)-(c) showed the comparison of ferroelectric properties i.e., remanent polarization (P_r), normalized coercive field (E_c/E_{max}) and loop squareness (R_{sq}) between (1-x)PZT–xBDT and (1-x)PZT–xBNbT systems. The result showed that an addition small amount of doped-BIT (x = 0.1) into PZT (0.9PZT–0.1BDT and 0.9PZT–0.1BNbT) enhanced ferroelectric properties of PZT ceramic, where increased remanent polarization, reduced coercive field and increased loop squareness were obtained. This seemed to be an influence of the highest density, better homogeneity of microstructure and doping effect. In the case of doping effect, it could be explained that doped-BIT content dissolved into PZT, according to X-ray diffraction analysis. This result attributed to Bi^{3+} or Dy^{3+} and Nb^{5+} ions of doped-BIT substituted at Pb^{2+} (A-site) and Zr^{4+}/Ti^{4+} (B-site) of PZT lattices, respectively. This thus acted as donor doping in the system, which was expected to reduce the concentration of oxygen vacancy and lead to a reduction in the concentration of domain stabilizing defect pairs. This resulted to an increase in domain wall mobility which then caused the increase in remanent polarization and reduce in coercive field. However, the 0.9PZT–0.1BNbT ceramic showed higher ferroelectric properties than 0.9PZT–0.1BDT ceramic. This result could be related to an effect of phase evolution. Namely, the 0.9PZT–0.1BNbT pattern showed only distorted tetragonal phase while 0.9PZT–0.1BDT pattern also presented a main peak of $Bi_4Ti_3O_{12}$ phase. It is known that the presence of any second phases is liable to generate non-ferroelectric phase caused reduce ferroelectric properties in this composition.

Figure 6.5(a)-(c) revealed that BNbT ceramic had better ferroelectric properties than those of BDT ceramic, i.e. higher remanet polarization, lower coercive field and higher loop squareness. This result could be directly related to the effect of different Bi or Ti site doping. Namely, the introduction of the Nb^{5+} at the Ti^{4+} (Ti-site) in $Bi_4Ti_3O_{12}$ as donor impurities can effectively reduce oxygen vacancies. A decrease of the oxygen vacancies resulted in the improved ferroelectric properties. The reason for an improvement of remanent polarization was due to the Nb^{5+} ion entered the Ti-site which had a larger ionic radius (0.64 Å) than the replaced Ti^{4+} ion (0.605 Å). This thus increased the structural distortion of oxygen octahedral, which was responsible for the change in remanent polarization value [49]. Moreover, the Nb content was a donor doping that caused the decrease in oxygen vacancies could be another factor affecting the remanent polarization. With the decrease of oxygen vacancies diffused to the domain wall in bulk, the pinning of domain wall decreased and the number of available switching domain wall decreased which resulted in the enhancement of remanent polarization and reduce the coercive field.

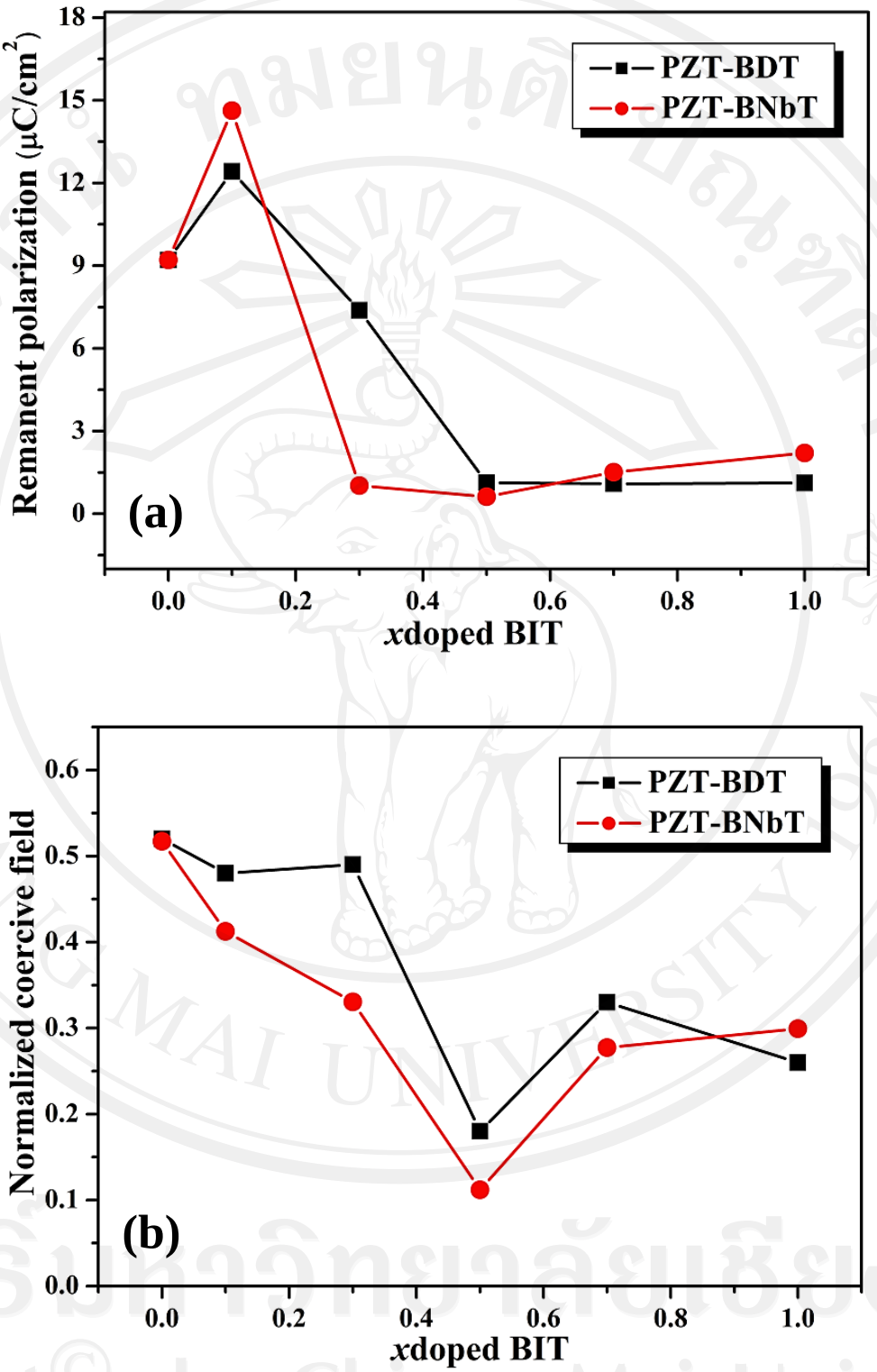

Figure 6.5 Comparison of ferroelectric properties (a) remanent polarization, (b) normalized coercive field and (c) loop squareness between (1-*x*)PZT–*x*BDT and (1-*x*) PZT–*x*BNbT systems.

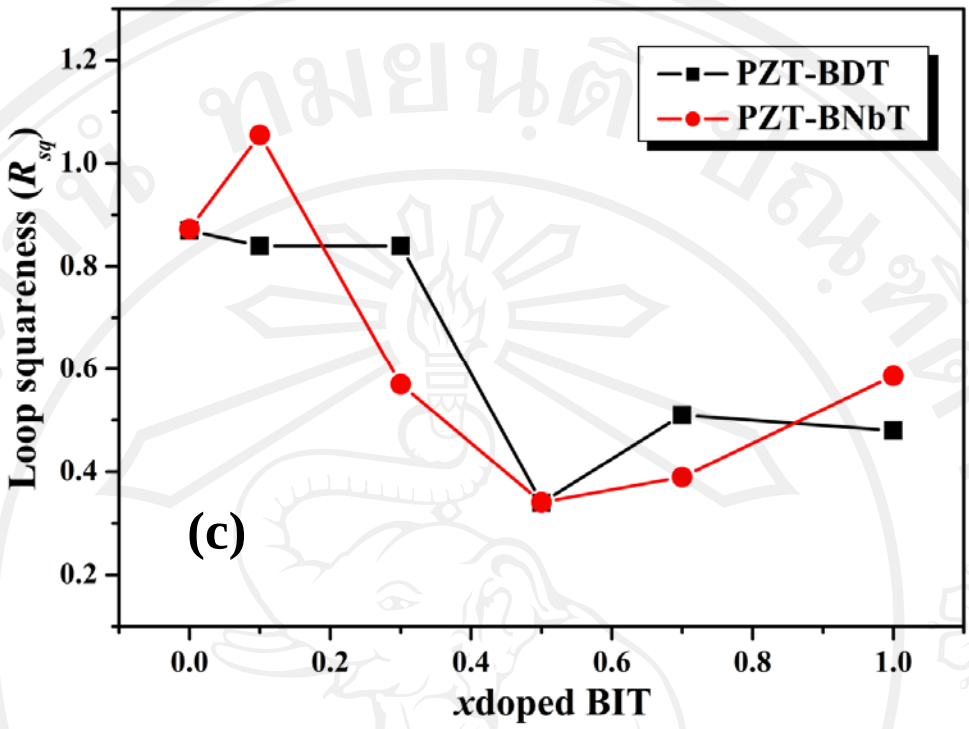

Figure 6.5 (continued) Comparison of ferroelectric properties (a) remanent polarization, (b) normalized coercive field and (c) loop squareness between (1-*x*)PZT–*x*BDT and (1-*x*)PZT–*x*BNbT systems.

6.5 Comparison of fatigue properties between PZT–BDT and PZT–BNbT systems

From fatigue properties of pure PZT ceramic, the dramatic drop of remanent polarization value was observed after electrical fatigue. The remanent polarization was decreased to 56% of the original value after 10^6 switching cycles. In the case of (1-*x*)PZT–*x*BDT and (1-*x*)PZT–*x*BNbT systems, they showed similar result. Namely, addition of doped-BIT content improved degradation of remanent polarization, as shown in Figure 6.6. This result revealed that PZT ceramic had severe polarization, agreed with other reports [74, 75, 135, 138].

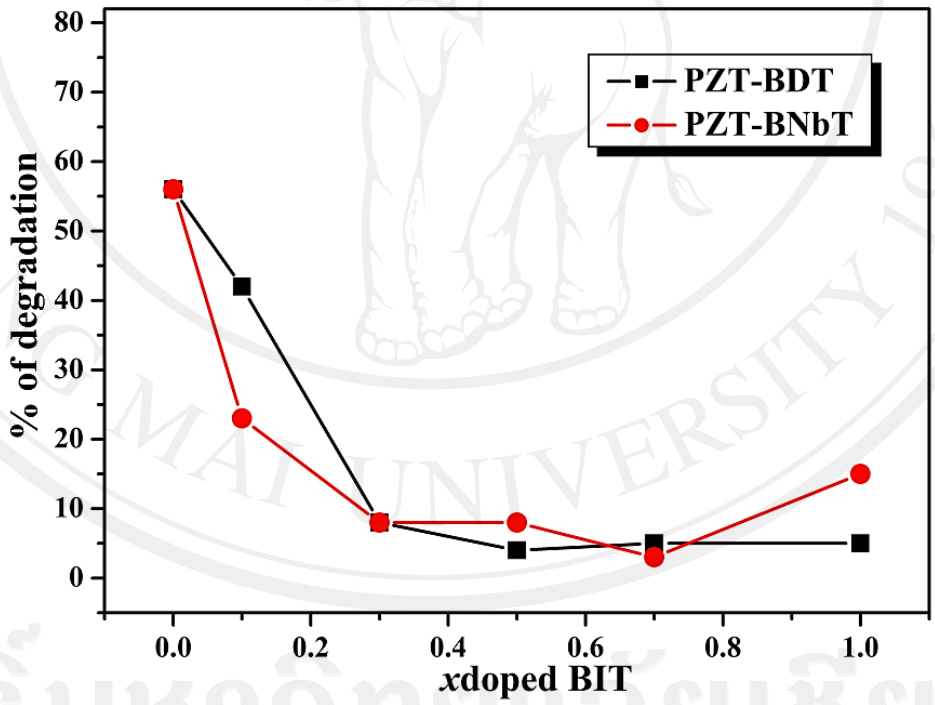

Figure 6.6 Comparison of the remanent polarization degraded between (1-*x*)PZT–*x*BDT and (1-*x*)PZT–*x*BNbT systems.

The comparison of fatigue properties between (1-*x*)PZT–*x*BDT and (1-*x*)PZT–*x*BNbT systems were also investigated in this section. Figure 6.7 showed plots of remanent polarization as a function of the number of switching cycles of BDT and BNbT ceramics. The result showed that BDT ceramic exhibited higher fatigue endurance than that of BNbT ceramic. It seemed to be the effect of Bi-site doping. Similar observations have been reported in other researches [8-13]. Failure characteristics of $Bi_4Ti_3O_{12}$ could be improved if some Bi ions (Bi-site) near the Ti-O octahedron layers were substituted with Dy^{3+} ions. This reason attributed that Dy doping suppressed the volatility of Bi and increased the stability of the metal-oxygen octahedral in $Bi_4Ti_3O_{12}$ [44]. Although, Bi and Dy ions have the same valence (+3), the different size of Bi^{3+} (1.03 Å) and Dy^{3+} (0.912 Å) might induce an addition distortion of lattice and further resulted in the potential barrier of oxygen vacancy change. Hence, the oxygen vacancy needed more energy to overcome this elevated potential barrier to jump and consequently pinned the domain wall. Therefore, the probability of oxygen vacancies diffusing to the domain wall decreased, lower probability of pinning the domain wall and caused the better fatigue property.

Addition of 10 wt% doped-BIT into PZT showed a degradation of remanent polarization after electrical fatigue (Figure 6.8). It seemed that fatigue endurance was improved at these compositions i.e. 0.9PZT–0.1BDT and 0.9PZT–0.1BNbT. This could be attributed to effect of the donor doping. It should be noted that oxygen vacancies in the PZT have an important influence on fatigue behavior [44, 139]. It was expected that the addition of donor dopants Bi^{3+} or Dy^{3+} and Nb^{5+} at A (Pb^{2+}) or B (Ti^{4+}) sites, respectively, reduced the oxygen vacancy concentration and caused a high stability through the switching cycles. However, 0.9PZT–0.1BDT showed lower

fatigue endurance than 0.9PZT–0.1BNbT ceramics. The responsible factor for the lower improvement in fatigue properties of 0.9PZT–0.1BDT was possibly a presence of second phase in the structure. The formation of secondary phase might alter the stoichiometric ratio of the original composition. Moreover, the poorer homogeneity of 0.9PZT–0.1BDT microstructure could be another factor. The structural inhomogeneity could produce traps of domain walls, thus reduced domain wall mobility. Increasing of doped-BIT content ≥ 30 wt% showed similar trend of fatigue endurance (Figure 6.9), where almost no change in ferroelectric values after electrical fatigue. This reason could be attributed to the increased of content of bi-layered compound.

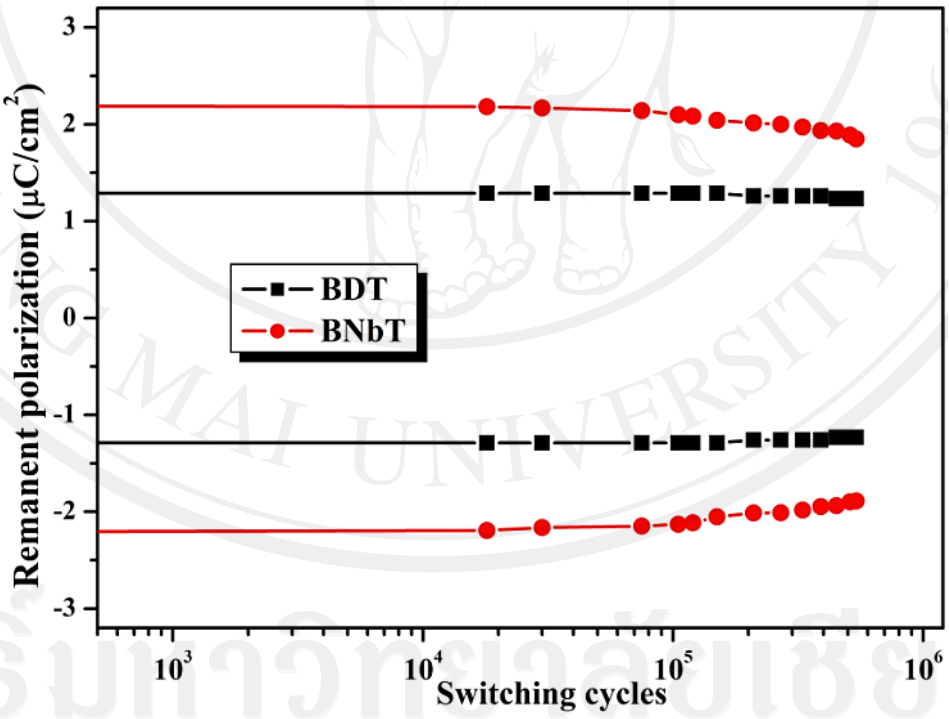

Figure 6.7 Comparison of fatigue behavior between BDT and BNbT ceramic.

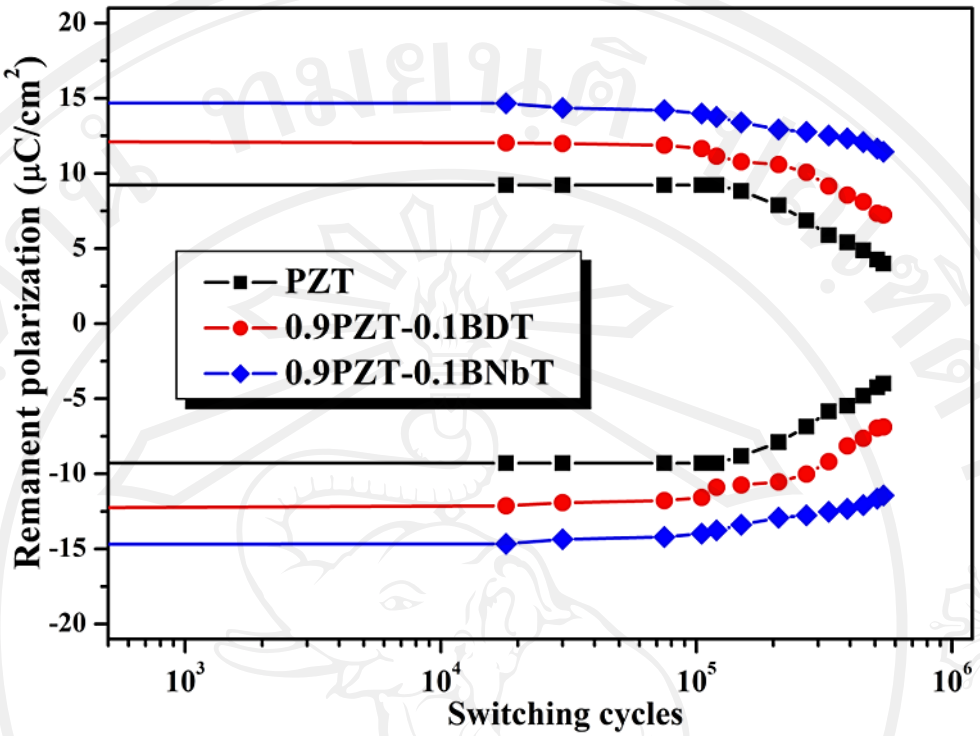

Figure 6.8 Comparison of fatigue behavior between PZT, 0.9PZT–0.1BDT and 0.9PZT–0.1BNbT ceramic.

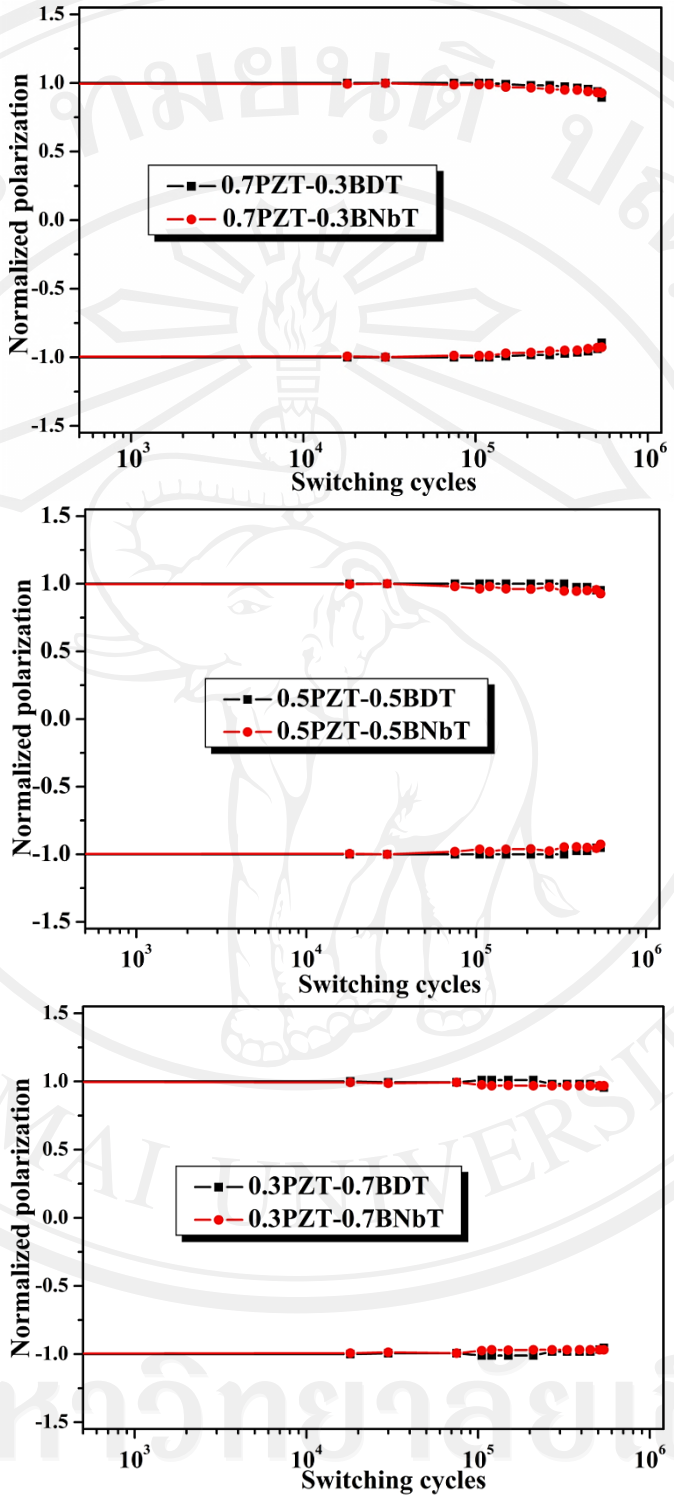

Figure 6.9 Comparison of fatigue behavior between (1-*x*)PZT–*x*BDT and (1-*x*)PZT–*x*BNbT (when *x* = 0.3, 0.5 and 0.7) ceramics.

From the comparison of various properties between (1-*x*)PZT–*x*BDT and (1-*x*) PZT–*x*BNbT systems, the results revealed that the optimum composition of these new ceramic systems could be obtained at $x = 0.1$, where higher densities, homogeneous of microstructure, increase in dielectric constant and increase in ferroelectric properties were achieved as summarized in Table 6.1.

Table 6.1 Comparison of properties between PZT, BDT, BNbT, 0.9PZT–0.1BDT and 0.9PZT–0.1BNbT ceramic

Composition	ρ (g/cm^3)	ε_r	tanδ	P_r (μC/cm^2)	P_{max} (μC/cm^2)	E_c/E_{max}	R_{sq}	% of degradation
PZT	7.63	929	0.018	9.26	12.88	0.52	0.87	56
BDT	7.60	130	0.028	1.31	4.42	0.26	0.84	5
BNbT	7.34	154	0.028	2.21	4.32	0.30	1.06	23
0.9PZT–0.1BDT	7.72	514	0.039	12.42	18.22	0.48	0.48	42
0.9PZT–0.1BNbT	7.75	731	0.022	14.62	19.31	0.41	0.58	15